Prompt photon production at HERA in the k_T-factorization approach

Nikolay P. Zotov

(SINP, Lomonosov Moscow State University)

in collaboration with
S.P. Baranov (Lebedev Physics Institute, Moscow)

A.V. Lipatov (SINP, Lomonosov Moscow State University)

DESY 10-024, arXiv:1001.4782 [hep-ph]

O U T L I N E

1. Introduction and motivations
2. Theoretical framework
3. Numerical results
4. Conclusions

1. Introduction and motivations

The production of prompt photons in deep inelastic ep collisions at HERA is a subject of the intense theoreticl and experimental studies.

Such processes provide a direct probe of the hard subprocess dynamics and the evolution in initial state, since the produced photons are largely insensitive to the effects of final-state hadronization.

Studying the photon production in deep inelastic scattering (DIS) provides a test of perturbative Quantum Chromodynamics (QCD) with two hard scales: E_T^γ, the transverse energy of the emitted photon, and Q^2, the exchanged photon virtuality. Understanding of the production dynamics is also important for searches of new particles decaying to photons at the LHC conditions.

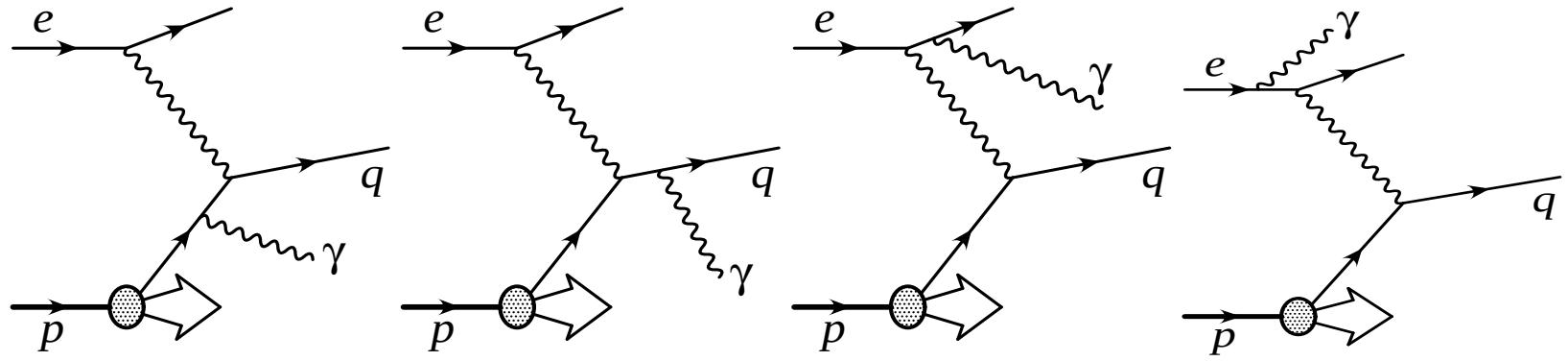

Figure 1:

At the leading-order of QCD, the production of the prompt photons in DIS is described by the parton subprocess $eq \to e\gamma q$.The corresponding cross section $\sigma(ep \to e\gamma X)$ can be obtained by convoluting the parton-level cross section $\hat{\sigma}(eq \to e\gamma q)$ with the quark distribution functions in a proton.

The observed final-state photon can be emitted by a quark or by a lepton (the so-called QQ and LL mechanisms). The interference contribution (LQ) is expected to be small.

The QQ mechanism includes the direct photon radiation from the quark line and also the so-called fragmentation processes, where the produced quark forms a jet containing a photon with large fraction of the jet energy. This contribution involves poorly known quark-to-photon fragmentation functions $f_{q\to\gamma}(z)$. However, the isolation criterion introduced in experimental analyses substantially reduces the fragmentation component.

Recently the H1 and ZEUS collaborations have reported their data on the deep inelastic production of prompt photon at HERA, both inclusive and in association with a hadronic jet.
The presented data on the inclusive prompt photon production

S. Chekanov et al. (ZEUS Collab.), arXiv:0909.4223 [hep-ex],

F.D. Aaron et al. (H1 Collab.), Eur. Phys. J. C54 (2008) 371.

have been compared with the LO pQCD $\mathcal{O}(\alpha^3)$ calculations.

A. Gehrmann-De Ridder, T. Gehrmann, E. Poulsen, Phys. Rev. Lett. 66 (2006) 132006.

Substantial (by a factor of about 2) disagreement between the data and theory has been found at low Q^2.

Also, the absolute size of reported experimental cross sections turned out to exceed also the predictions of MC generators HERWIG and PYTHIA (by the factors of 7.9 and 2.3, respectively).
Comparison between the LO pQCD calculations and the data in bins of η^γ shows that the difference can be attributed mainly to the underestimation of the QQ contribution.

Concerning the higher-order corrections, the next-to-leading order (NLO) $\mathcal{O}(\alpha^3\alpha_s)$ predictions are available for the associated photon plus jet phase space selection only, yet not for inclusive process. These predictions are higher than the results of LO calculations, especially at low Q^2, but still underestimate the data.

Here we use the k_T-factorization approach, which is based on the BFKL or CCFM evolution equations for u.g.d. In this approach, the large logarithm terms proportional to $\ln s \sim \ln 1/x$ are summed up to all orders of perturbation theory (in the leading logarithm approximation) and the transverse momentum k_T of the incoming partons is taken into account.

We have applied this approach to the inclusive and jet associated prompt photon photo- and hadroproduction at HERA and the Tevatron.
As it was demonstrated also in the ZEUS paper and also in the recent study performed by the H1 Collaboration, the k_T-factorization predictions are in better agreement with the data than collinear NLO calculations:

S. Chekanov et al. (ZEUS Collab.), Eur. Phys. J. C49 (2007) 511,
F.D. Aaron et al. (H1 Collab.), arXiv:0910.5631 [hep-ex].

Here we extend our previous study to the DIS region. We calculate the relevant off-shell (i.e. k_T-dependent) amplitude $\mathcal{M}(eq^* \to e\gamma q)$, where the virtuality of the incoming quarks is properly taken into account. Our consideration covers both the LL and QQ production mechanisms. We neglect the LQ mechanim since it gives only about 3% contribution to the total cross section. The unintegrated quark and gluon densities in a proton $f_{q,g}(x, \mathbf{k}_T^2, \mu^2)$ are taken in the Kimber-Martin-Ryskin (KMR) form:

M.A. Kimber, A.D. Martin, M.G. Ryskin, Phys. Rev. D63 (2001) 114027;
G. Watt, A.D. Martin, M.G. Ryskin, Eur. Phys. J. C31 (2003) 73.

2. Theoretical framework

2.1 Off-shell amplitude of the $eq^* \to e\gamma q$ subprocesses.

Let us start with the LL production mechanism. There are two simple Feynman diagrams which describe this partonic subprocess at the leading order in $\alpha_{\rm em}$. The relevant matrix element reads

$$\mathcal{M}_{LL}(eq^* \to e\gamma q) = e_q e^3 \epsilon^\mu_\lambda \frac{1}{q^2} L^{\mu\nu} H^\nu.$$

The leptonic and hadronic tensors are given by the following expressions:

$$L^{\mu\nu} = \bar{u}(p_{e'}) \left[\gamma^\mu \frac{\hat{p}_{e'} + \hat{p}_\gamma + m_e}{(p_{e'} + p_\gamma)^2 - m_e^2} \gamma^\nu + \gamma^\nu \frac{\hat{p}_e - \hat{p}_\gamma + m_e}{(p_e - p_\gamma)^2 - m_e^2} \gamma^\mu \right] u(p_e),$$

$$H^\nu = \bar{u}(p_q) \gamma^\nu u(k),$$

where k, p_q, p_γ are the four-momenta of the initial, final quarks and the outgoing photon.

The summation over the photon polarizations is carried with $\Sigma\epsilon^\mu\epsilon^\nu = g^{\mu\nu}$, and the spin density matrix for on-shell spinores is taken in the standarrd form $u(p)\bar{u}(p) = \hat{p} + m$. In the case of initial off-shell quarks the original on-shell spin density matrix has to be substitute for different expression.

The expression for $|\bar{\mathcal{M}}_{QQ}(eq^* \to e\gamma q)|^2$ can be easily obtained from previous expressions if we replace $p_e \to k$, $p_{e'} \to p_q$, $k \to p_e$, $p_q \to p_{e'}$ and multiply first m.e by an extra factor e_q. In massless limit, the squared off-shell matrix elements $|\bar{\mathcal{M}}_{LL,QQ}(eq^* \to e\gamma q)|^2$ summed over the final states and averaged over the initial ones are

$$|\bar{\mathcal{M}}_{LL}|^2 = \frac{(4\pi\alpha_{em})^3 e_q^2\, x}{16(k^2 - 2(p_q\cdot k))^2}\left[\frac{F_{LL}^{(1)}}{(p^\gamma\cdot p_{e'})^2} + \frac{F_{LL}^{(2)}}{(p^\gamma\cdot p_e)^2} + \frac{2F_{LL}^{(12)}}{(p^\gamma\cdot p_e)(p^\gamma\cdot p_{e'})}\right],$$

$$|\bar{\mathcal{M}}_{QQ}|^2 = \frac{(4\pi\alpha_{em})^3 e_q^4\, x}{64(p_e\cdot p_{e'})^2}\left[\frac{F_{QQ}^{(1)}}{(p^\gamma\cdot p_q)^2} + \frac{F_{QQ}^{(2)}}{((p^\gamma\cdot k) - k^2)^2} + \frac{2F_{QQ}^{(12)}}{(p^\gamma\cdot p_q)((p^\gamma\cdot k) - k^2)}\right].$$

2.2 Cross section for the prompt photon production.

In the $k_T$factorization approach

$$\sigma_{LL,QQ}(ep \to e\gamma X) = \sum_q \int \frac{1}{256\pi^3 x^2 s\sqrt{s}|\mathbf{p}_{\gamma\,T}|\exp(y_\gamma)} |\bar{\mathcal{M}}_{LL,QQ}(eq^* \to e\gamma q)|^2 \times$$
$$\times f_q(x, \mathbf{k}_T^2, \mu^2) d\mathbf{p}_{e'\,T}^2 d\mathbf{p}_{q\,T}^2 d\mathbf{k}_T^2 dy_{e'} dy_q \frac{d\phi_{e'}}{2\pi}\frac{d\phi_q}{2\pi}\frac{d\phi}{2\pi},$$

where $y_{e'}$, y_q and $\phi_{e'}$ and ϕ_q are the center-of-mass rapidities and azimuthal angles of the outgoing electron and (anti)quark. The rapidity y_γ of the produced photon is given by

$$y_\gamma = \ln\left[\frac{\sqrt{s} - m_{e'\,T}\exp(y_{e'}) - m_{q\,T}\exp(y_q)}{|\mathbf{p}_{\gamma\,T}|}\right],$$

where $m_{e'\,T}$ and $m_{q\,T}$ are the transverse masses of the corresponding particles. We note that averaging the expression for σ over ϕ and taking the limit $\mathbf{k}_T^2 \to 0$ we recover the well-known LO result of collinear parton model.

We used the unintegrated quark densities in a proton $f_q(x, \mathbf{k}_T^2, \mu^2)$, which taken in the KMR form. In KMR formalism the u. p. (quark and gluon) d. are constructed from the known pdf $xa(x, \mu^2)$, where $a = g$ or $a = q$. For the input, we used the recent leading-order Martin-Stirling-Thorne-Watt (MSTW) pdf from

A.D. Martin, W.J. Stirling, R.S. Thorne, G. Watt, Eur. Phys. J. C63 (2009) 189.

We choosed the renormalization and factorization scales to be $\mu^2 = \xi Q^2$ and varied the scale parameter ξ between 1/2 and 2 about the default value $\xi = 1$. We used the LO formula for $\alpha_s(\mu^2)$ with $n_f = 4$ active (massless) quark flavours and $\Lambda_{\rm QCD} = 200$ MeV, such that $\alpha_s(M_Z^2) = 0.1232$.

2.3 Fragmentation contribution.

We do not use the conception of f.f. evidently. But the perturbation theory becomes nonapplicable when the wavelength of the emitted photon (in the emitting quark rest frame) becomes larger then the typical hadronic scale $\mathcal{O}$ (1 GeV^{-1}). Then the nonperturbative effects of hadronization or fragmentation must be taken into account. Accordingly, the calculated cross section can be split into two pieces

$$d\sigma = d\sigma_{\rm direct}(\hat{\mu}^2) + d\sigma_{\rm fragm}(\hat{\mu}^2)$$

with $d\sigma_{\rm direct}(\hat{\mu}^2)$ representing the perturbative contribution and $d\sigma_{\rm fragm}(\hat{\mu}^2)$ the fragmentation contribution. In our calculations we choose the fragmentation scale $\hat{\mu}^2$ to be the invariant mass of the quark + photon subsystem,$\hat{\mu}^2 = (p+p_i)^2$, and restrict $d\sigma_{\rm direct}(\hat{\mu}^2)$ to $\hat{\mu} \geq M \simeq 1$ GeV. Under this condition, the contribution $d\sigma_{\rm direct}(\mu^2)$ is free from divergences. We have checked that the sensitivity of our results to the choice of M is reasonably soft.
As far as the fragmentation contribution is concerned, its size is dramatically reduced by the photon isolation cuts.

2.4 Photon isolation cuts.

In order to reduce huge background from the secondary photons produced by the decays of π^0 and η mesons the isolation criterion is introduced in the experimental analyses. A photon is isolated if the amount of hadronic transverse energy $E_T^{\rm had}$, deposited inside a cone with aperture R centered around the photon direction in the pseudorapidity and azimuthal angle plane, is smaller than some value $E_T^{\rm max}$:

$$\sum_{\rm had} E_T^{\rm had} \leq E_T^{\rm max},$$

$$(\eta^{\rm had} - \eta)^2 + (\phi^{\rm had} - \phi)^2 \leq R^2.$$

Both the H1 and ZEUS collaborations take $R \sim 1.0$ and $E_T^{\rm max} \sim 1$ GeV. Isolation not only reduces the background from light hadron decays but also significantly reduces the fragmentation components connected with collinear photon radiation. It was shown that after applying the these isolation cuts the contribution from the fragmentation subprocesses is strongly suppressed.

3. Numerical results

3.1 Inclusive production

Our calculations of the total cross sections give $47.7^{+1.3}_{-1.5}$ pb, $6.1^{+0.3}_{-0.3}$ pb and $22.0^{+0.7}_{-0.9}$ pb for the H1, ZEUS [1] and ZEUS [2] kinematical regions, respectively. The experimentally measured cross sections are $50.3 \pm 1.7\,(\text{stat.})\,^{+6.8}_{-7.8}\,(\text{syst.})$ pb, $5.64 \pm 0.58\,(\text{stat.})\,^{+0.47}_{-0.72}\,(\text{syst.})$ pb and $19.4 \pm 0.7\,(\text{stat.})\,^{+1.2}_{-1.0}\,(\text{syst.})$ pb.The collinear LO pQCD predictions are 28.6 pb and 5.39 pb for the H1 and ZEUS kinematical regions.
Besides that, the sole QQ contribution has been extracted in the ZEUS experiment [2] giving $12.2 \pm 0.7\,(\text{stat.})\,^{+1.2}_{-1.0}\,(\text{syst.})$ pb. Our prediction of $14.8^{+0.4}_{-0.5}$ pb is very close to this value. We find that the QQ contribution yelds about 65% of the total cross section. In the collinear LO calculations this mechanism gives only about 50%. According to the observation of ZEUS Collab., the difference between the collinear LO calculations and the data can mainly be attributed to an underestimation of the QQ contribution.

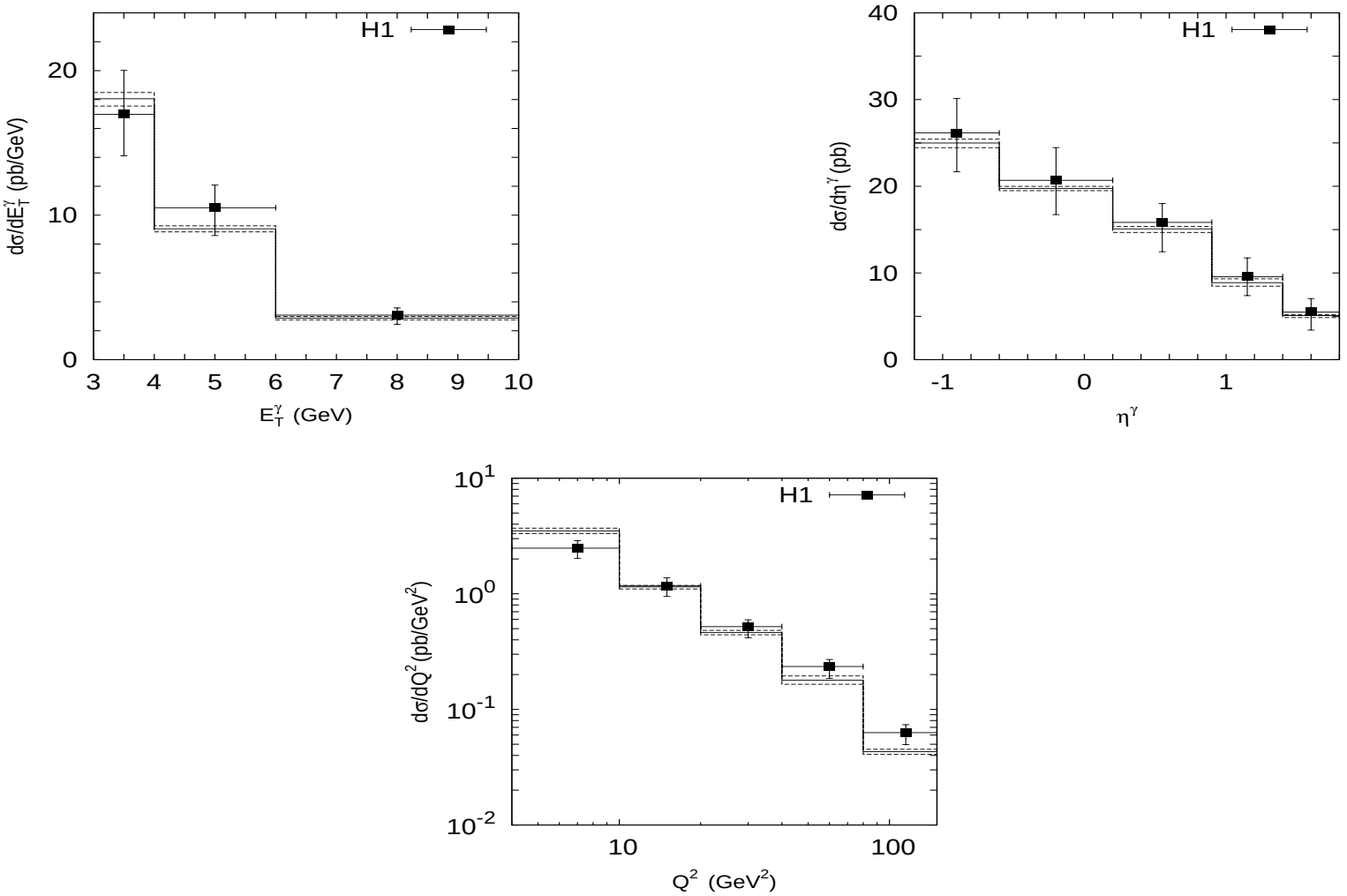

Figure 2: *Differential cross sections of the inclusive deep inelastic prompt photon production as a function of* E_T^γ, η^γ *and* Q^2 *calculated at* $3 < E_T^\gamma < 10$ *GeV*, $-1.2 < \eta^\gamma < 1.8$, $4 < Q^2 < 150$ GeV^2, $E'_e > 10$ *GeV*, $153^o < \theta'_e < 177^o$, $y > 0.05$ *and* $W_X > 50$ *GeV. The solid histogram corresponds to the default scale* $\mu^2 = Q^2$, *the upper and lower dashed histograms correspond to variation of scale.*

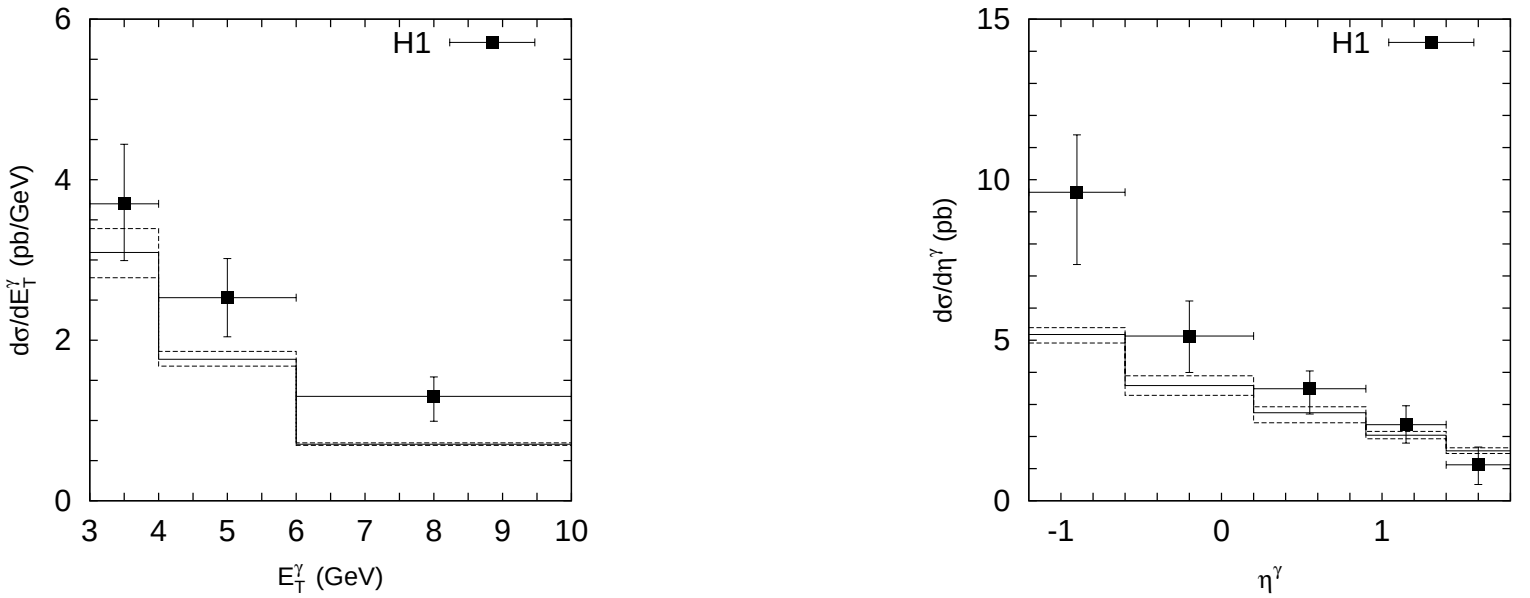

Figure 3: *Differential cross sections of the deep inelastic inclusive prompt photon production as a function of* E_T^γ *and* η^γ *calculated at* $3 < E_T^\gamma < 10$ *GeV*, $-1.2 < \eta^\gamma < 1.8$, $40 < Q^2 < 150$ GeV^2, $E'_e > 10$ *GeV*, $153^\circ < \theta'_e < 177^\circ$, $y > 0.05$ *and* $W_X > 50$ *GeV. Notation of the histograms is as in Fig. 2.*

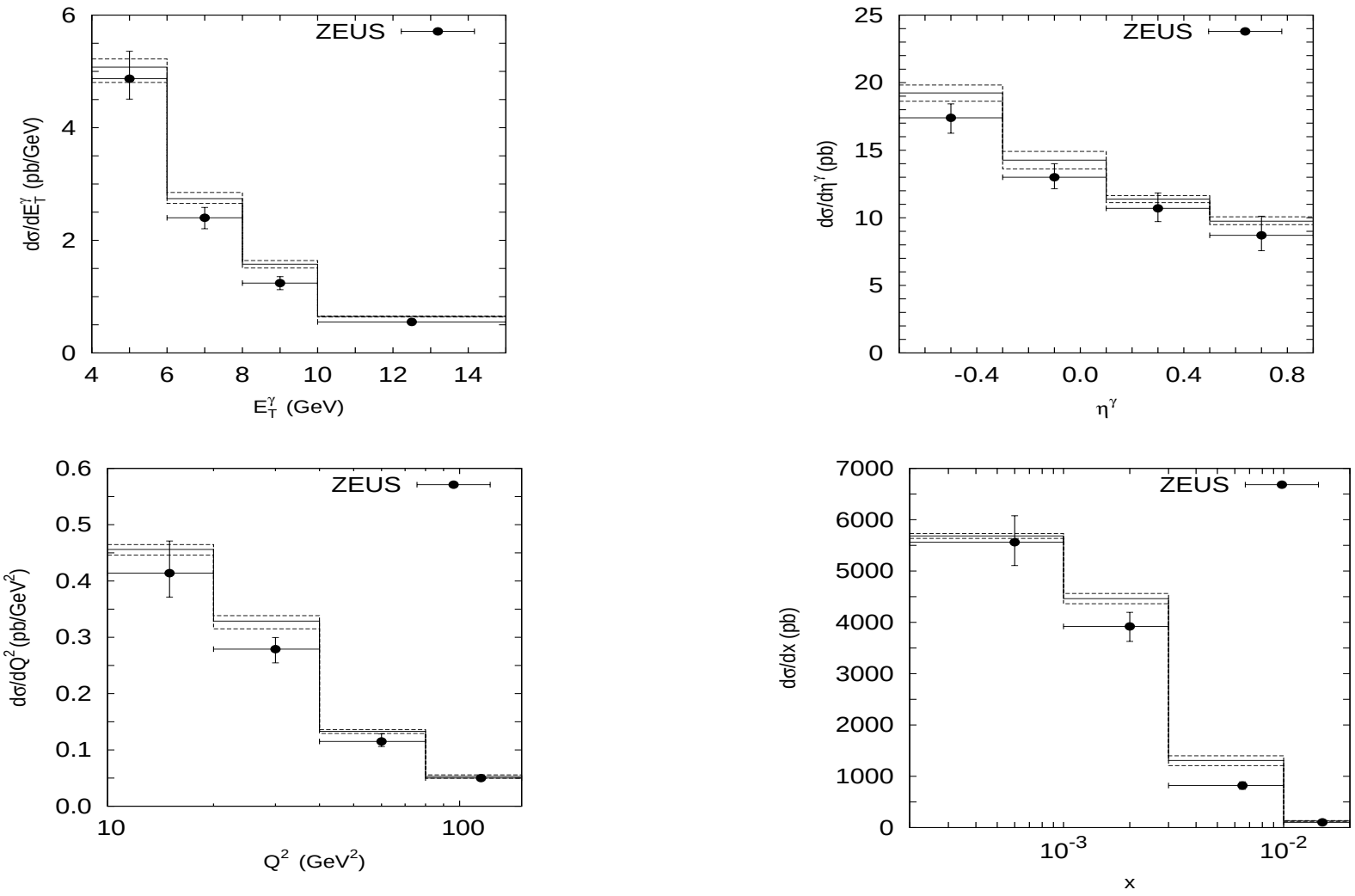

Figure 4: *Differential cross sections of the inclusive deep inelastic prompt photon production at HERA as a function of* E_T^γ, η^γ, Q^2 *and* x *calculated at* $4 < E_T^\gamma < 15$ *GeV*, $-0.7 < \eta^\gamma < 0.9$, $10 < Q^2 < 350$ *GeV*^{2}, $E'_e > 10$ *GeV*, $139.8^\circ < \theta'_e < 171.9^\circ$ *and* $W_X > 5$ *GeV. Notation of the histograms is as in Fig. 2.*

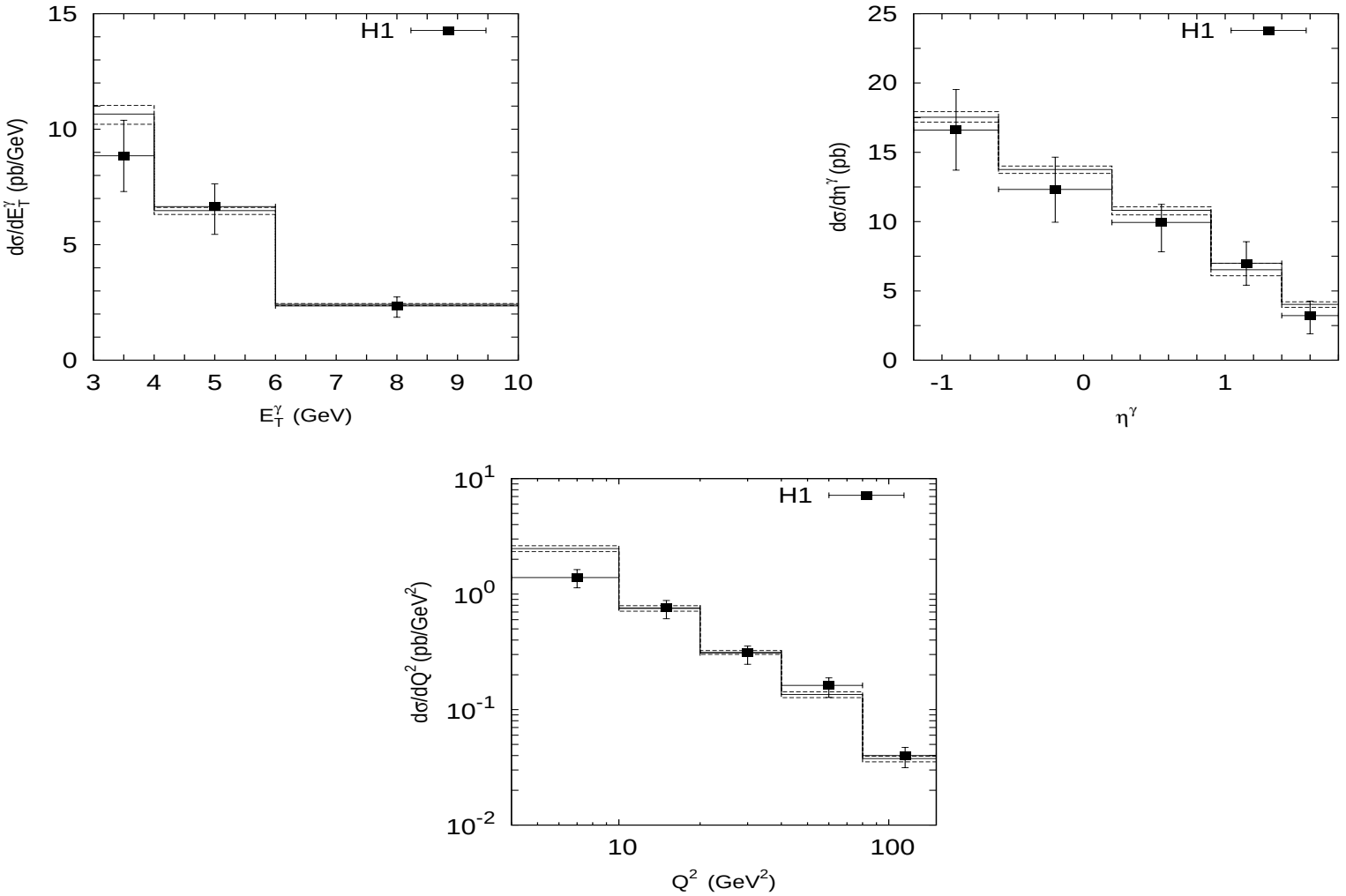

Figure 5: *Differential cross sections of the deep inelastic prompt photon and jet associated production as a function of* E_T^γ, η^γ *and* Q^2 *calculated at* $3 < E_T^\gamma < 10$ *GeV*, $E_T^{\rm jet} > 2.5$ *GeV*, $-1.2 < \eta^\gamma < 1.8$, $-1.0 < \eta^{\rm jet} < 2.1$, $4 < Q^2 < 150$ *GeV*^{2}, $E'_e > 10$ *GeV*, $153^{\rm o} < \theta'_e < 177^{\rm o}$, $y > 0.05$ *and* $W_X > 50$ *GeV. Notation of the histograms is as in Fig. 2.*

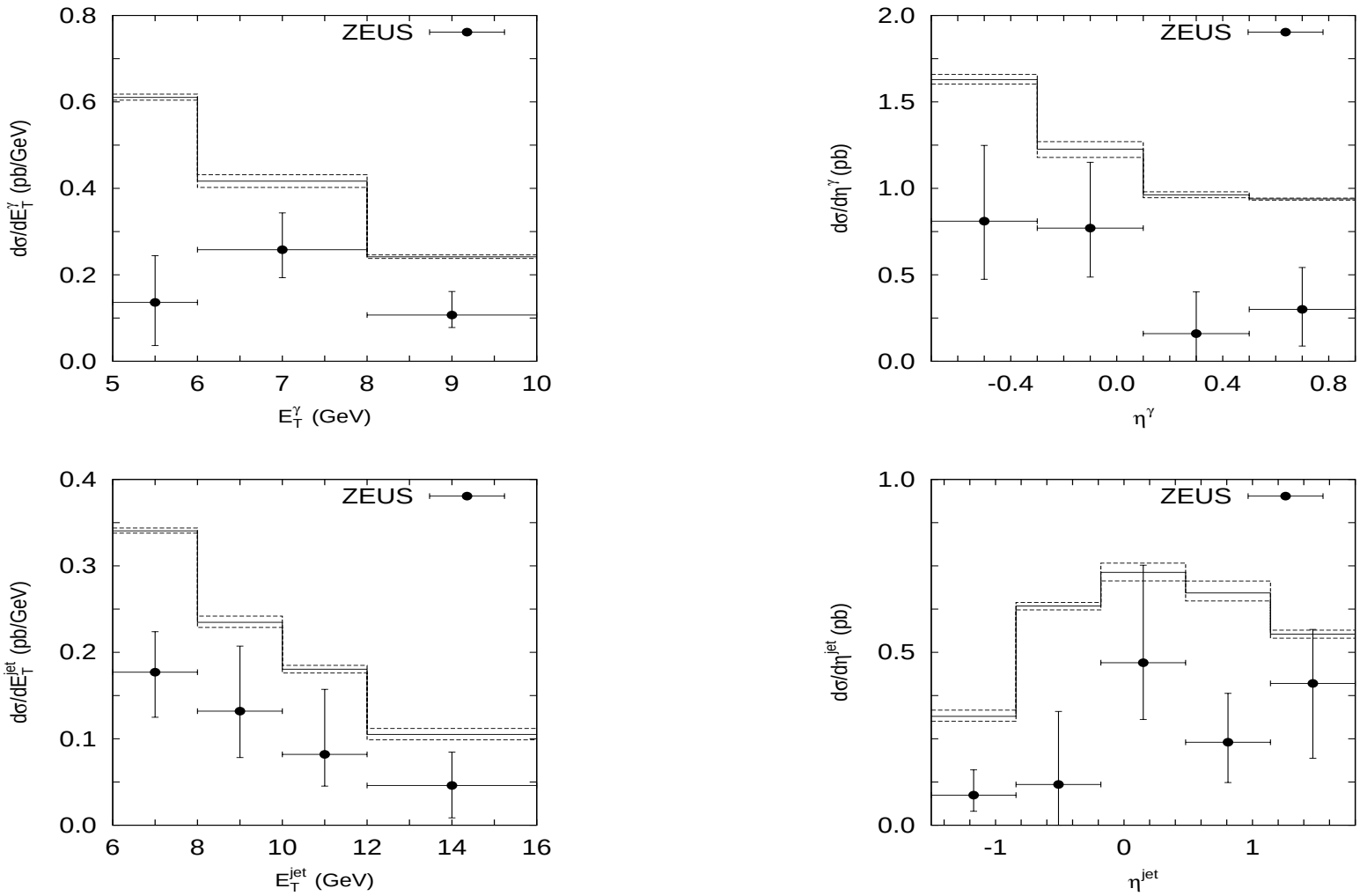

Figure 6: *Differential cross sections of the deep inelastic prompt photon and jet associated production as a function of* E_T^γ, η^γ, $E_T^{\rm jet}$ *and* $\eta^{\rm jet}$ *calculated at* $5 < E_T^\gamma < 10$ *GeV*, $E_T^{\rm jet} > 6$ *GeV*, $-0.7 < \eta^\gamma < 0.9$, $-1.5 < \eta^{\rm jet} < 1.8$, $Q^2 > 35$ *GeV*^{2}, $E'_e > 10$ *GeV and* $139.8^{\rm o} < \theta'_e < 171.8^{\rm o}$. *Notation of the histograms is as in Fig. 2.*

3.2 Prompt photon production in association with jet

One can see that the distributions measured by the H1 Collaboration are well reproduced by our calculations. However, our results overeshoot the ealier ZEUS data.

The collinear NLO predictions describe well the shapes of the differential c.s. $d\sigma/dE_T^\gamma$, $d\sigma/d\eta^\gamma$ **and** $d\sigma/dQ^2$, **but the normalization is too low, by about** 40%. **The difference between the LO and NLO predictionsis mostly concentrated at low** Q^2.
The calculated total c.s. $\sigma(ep \to e\gamma + \text{jet}) = 33.2^{+0.9}_{-1.0}$ **pb and** $1.9^{+0.1}_{-0.1}$ **pb have to be compared with** $31.6 \pm 1.2\,(\text{stat.})\,^{+4.2}_{-4.8}\,(\text{syst.})$ **pb and** $0.86 \pm 0.14\,(\text{stat.})\,^{+0.44}_{-0.34}\,(\text{syst.})$ **pb, measured by the H1 and ZEUS collaborations in the relevant kinematical regions.**
The total c.s. calculated in the collinear approximation at the LO and NLO level for H1 conditions are 16.7 pb and 20.2 pb, respectively.

3. Conclusions

- **We have investigated the deep inelastic production of prompt photons at HERA in the k_T-factorization approach, inclusive and jet associated production.**
- **Our study is based on the off-shell m.e. $eq^* \to e\gamma q$ and the KMR unintegrated quark densities in a proton.**
- **Our numerical predictions on inclusive production cross sections are in well agreement with the H1 and ZEUS data.**
- **We have demonstrated that in the k_T-factorization approach the role of the QQ contribution is enhanced compared to the collinear LO approximation of QCD.**
- **Our results for jet associated production agree with the H1 measurements but overshoot the ZEUS data.**

Backup slides

Let us consider the off-shell quark line as internal line in the "extended" diagram. Let the initial on-shell quark with four-momentum p and mass m_q radiates a quantum (photon or gluon) and becomes an off-shell quark with four-momentum k. So, for the extended diagram squared we write:

$$|\mathcal{M}|^2 \sim \mathrm{Sp}\left[\bar{\mathcal{T}}^\mu \frac{\hat{k}+m_q}{k^2-m_q^2}\,\gamma^\nu\, u(p)\bar{u}(p)\,\gamma_\nu \frac{\hat{k}+m_q}{k^2-m_q^2}\,\mathcal{T}_\mu\right],$$

where $\mathcal{T}$ is the rest of the original matrix element which remains unchanged. The expression presented between $\bar{\mathcal{T}}^\mu$ and $\mathcal{T}_\mu$ now plays the role of the off-shell quark spin density matrix. Using the on-shell condition $u(p)\,\bar{u}(p) = \hat{p} + m_q$ and performing the Dirac algebra one obtains in the massless limit $m_q \to 0$:

$$|\mathcal{M}|^2 \sim \frac{1}{(k^2)^2}\bar{\mathcal{T}}^\mu \left(2k^2\hat{p} - 4(p\cdot k)\hat{k}\right)\mathcal{T}_\mu.$$

Now we use the Sudakov decomposition $k = xp + k_T$ and neglect

the second term in the parentheses of last formula in the small-x limit to arrive at

$$|\mathcal{M}|^2 \sim \frac{2}{xk^2}\bar{\mathcal{T}}^\mu \, x\hat{p} \, \mathcal{T}_\mu .$$

(Essentially, we have neglected here the negative light-cone momentum fraction of the incoming quark). The properly normalized off-shell spin density matrix is given by $x\hat{p}$, while the factor $2/xk^2$ has to be attributed to the quark distribution function (determining its leading behavior). With this normalization, we successfully recover the on-shell collinear limit when k is collinear with p.